Since January 2020 Elsevier has created a COVID-19 resource centre with free information in English and Mandarin on the novel coronavirus COVID-19. The COVID-19 resource centre is hosted on Elsevier Connect, the company's public news and information website.

International Journal of Biological Macromolecules 163 (2020) 1787–1797

Contents lists available at ScienceDirect

International Journal of Biological Macromolecules

journal homepage: http://www.elsevier.com/locate/ijbiomac

Prediction of potential inhibitors for RNA-dependent RNA polymerase of SARS-CoV-2 using comprehensive drug repurposing and molecular docking approach

Md. Sorwer Alam Parvez [a,1], Md. Adnan Karim [b,f,1], Mahmudul Hasan [c,1], Jomana Jaman [d], Ziaul Karim [e], Tohura Tahsin [a], Md. Nazmul Hasan [b], Mohammad Jakir Hosen [a,*]

[a] Department of Genetic Engineering & Biotechnology, Shahjalal University of Science & Technology, Sylhet 3114, Bangladesh
[b] Department of Genetic Engineering & Biotechnology, Jashore University of Science & Technology, Jashore, Bangladesh
[c] Department of Pharmaceuticals and Industrial Biotechnology, Sylhet Agricultural University, Sylhet 3100, Bangladesh
[d] Department of Biotechnology, Bangladesh Agricultural University, Mymensingh, Bangladesh
[e] Department of Biology, Chemistry and Pharmacy, Free University of Berlin, Berlin, Germany
[f] Center for Bioinformatics, Universitat Des Saarlandes, Saarbrucken, Germany

ARTICLE INFO

Article history:
Received 27 June 2020
Received in revised form 24 August 2020
Accepted 14 September 2020
Available online 17 September 2020

Keywords:
COVID-19
SARS-CoV-2
RNA-dependent RNA polymerase
Drug

ABSTRACT

The pandemic prevalence of COVID-19 has become a very serious global health issue. Scientists all over the world have been seriously attempting in the discovery of a drug to combat SARS-CoV-2. It has been found that RNA-dependent RNA polymerase (RdRp) plays a crucial role in SARS-CoV-2 replication, and thus could be a potential drug target. Here, comprehensive computational approaches including drug repurposing and molecular docking were employed to predict an effective drug candidate targeting RdRp of SARS-CoV-2. This study revealed that Rifabutin, Rifapentine, Fidaxomicin, 7-methyl-guanosine-5′-triphosphate-5′-guanosine and Ivermectin have a potential inhibitory interaction with RdRp of SARS-CoV-2 and could be effective drugs for COVID-19. In addition, virtual screening of the compounds from ZINC database also allowed the prediction of two compounds (ZINC09128258 and ZINC09883305) with pharmacophore features that interact effectively with RdRp of SARS-CoV-2, indicating their potentiality as effective inhibitors of the enzyme. Furthermore, ADME analysis along with analysis of toxicity was also undertaken to check the pharmacokinetics and drug-likeness properties of the two compounds. Comparative structural analysis of protein-inhibitor complexes revealed that the amino acids Y32, K47, Y122, Y129, H133, N138, D140, T141, S709 and N781 are crucial for drug surface hotspot in the RdRp of SARS-CoV-2.

1. Introduction

The pandemic Corona Virus Disease 19 (COVID-19) has become a critical, rapidly emerging public health issue for the world. It is caused by the outbreak of Severe Acute Respiratory Syndrome Corona Virus 2 (SARS-CoV-2), and the disease characterized by fever, cough, severe shortness of breathing, nausea, vomiting and diarrhea [1]. As of 24 August 2020, SARS-CoV-2 infection has been reported in 188 countries with 23.4 million confirmed cases and 808,000 total deaths [2,3]. Epidemiological data have determined person to person transmission as the route of the rapid outbreak of COVID-19, which has become a major obstruction in combating the virus [4,5]. Clinical studies reported that older patients have a higher case of fatality rate (CFR) than the young, and males have a higher CFR than female [6]. Apart from acute respiratory distress, COVID-19 patients have been diagnosed with higher rate of renal impairment, indicating the development of kidney dysfunction [7]. Unfortunately, there are no proven drugs, vaccines or therapies available to fight against COVID-19.

SARS-CoV-2 is an enveloped, positive-sense, single-stranded RNA virus similar to SARS and MERS (Middle East Respiratory Syndrome) coronavirus [8]. Along with structural proteins (like spike glycoprotein and accessory proteins), the viral genome also encodes non-structural proteins, including 3-chymotrypsin-like protease, papain-like protease, helicase and RNA-dependent RNA polymerase (RdRp) [9]. RdRp is an essential enzyme involved in the replication of RNA viruses including SARS-CoV-2. Several anti-viral drugs have been developed targeting this enzyme for treating infections like Hepatitis C, Zika and other coronaviruses [10]. Although not yet extensively explored, some of

* Corresponding author at: Department of Genetic Engineering & Biotechnology, Shahjalal University of Science & Technology, Sylhet 3114, Bangladesh.
E-mail addresses: sorwersust@yahoo.com (M.S.A. Parvez), jakir-gen@sust.edu (M.J. Hosen).
[1] Joint first author. Authors contributed equally.

https://doi.org/10.1016/j.ijbiomac.2020.09.098
0141-8130/

these drugs also target the SARS-CoV-2 RdRp or its catalyzed polymerization process [11–14]. A recent study suggested that two known antiviral drugs, Remdesivir and Favipiravir, which are used for the treatment of a variety of RNA virus diseases by targeting RNA polymerase and RdRp respectively, could successfully inhibit SARS-CoV-2 replication *in vitro* [13–17]. Unfortunately, the mechanism of action and the efficacy of these compounds remain unclear.

Computation biology and molecular docking approach have a wide variety of applications in drug discovery, giving novel insights to the screening of potential drugs for the treatment of COVID-19. These approaches also aid the understanding of the protein-ligand interactions as well as in figuring out drug surface hotspot, which are important for the discovery of an effective drug [18,19]. In addition, drug repurposing approach is used for the identification of existing drugs for one disease, for the treatment of another disease. As the long-term solution, vaccine, will take years to be marketable, effective repurposing of existing drug remains the only alternative way to fight against an emerging disease like COVID-19 [20–23]. Thus, in the presented study, drugs with proven anti-viral activity were analyzed using molecular docking and pharmacophore modeling technique to target RdRp of SARS-CoV-2. Our findings can open a new avenue to fight against COVID-19.

2. Materials and methods

2.1. Retrieval of the structure of SARS-CoV-2 RNA polymerase and drug candidates list

The RdRp structure of SARS-CoV-2 was retrieved from the Protein Data Bank (PDB) with PDB ID: 6M71 [24]. Furthermore, 44 drug candidates having inhibitory activity against RNA polymerase were selected by comprehensive literature study, and their PDB structures were retrieved from the Drug Bank Database (Supplementary Table 1) [25]. RdRp inhibitor drugs were prioritized; but drugs that are DNA-dependent RNA polymerase inhibitors having the antiviral activity were also included.

2.2. Screening of RNA polymerase inhibitors against the RdRp of SARS-CoV-2

The AutoDock Vina software of molecular docking approaches was employed for the screening of the drugs against RdRp of SARS-CoV-2 [26]. At first, the crystal structure of RdRp was retrieved from the PDB, processed by removing water and complex molecules using PyMOL [27]. After preparing the PDB structures of the inhibitors, they were exposed to the RdRp polymerase of SARS-CoV-2 for analyzing the lowest binding energy and interactive amino acids. The grid box parameters were set to size 80 Å × 95 Å × 95 Å (x, y and z) and centre 121.253 Å × 121.376 Å × 120.149 Å (x, y and z). The 2D ligand-protein interaction diagrams were generated by LigPlot+ to find out the involved amino acids with their interactive position in the docked molecule [28]. Discovery Studio and PyMOL were used to visualize and analyze the ligand molecules' interactions with the viral proteins [29]. Additionally, the Protein-Ligand Interaction Profiler (PLIP) was also used to analyze the total number of non-covalent interactions (hydrogen bonds, water bridges, salt bridges, halogen bonds, hydrophobic interactions, π-stacking, π-cation interactions and metal complexes) in protein-ligand complexes [30].

2.3. Structural insights of drug surface hotspot in the RdRp of SARS-CoV-2

LigPlot+, Discovery Studio and PyMOL were used to figure out the drug surface hotspot from the docked structures of RdRp with the top-most polymerase inhibitors. Remdesivir and Favipiravir were used as positive control, as they were reported to be effective for COVID-19 by several recent studies [13,14].

2.4. Pharmacophore modeling and virtual screening of ZINC database

PharmaGIST was used for the modeling of the pharmacophore features that are essential for the interaction of RNA polymerase inhibitors with RdRp of SARS-CoV-2. In this study, the top-most inhibitors along with Remdisivir were used for the pharmacophore modeling [31,32]. ZINCPharmer was used to import the generated pharmacophore from PharmaGISTfor the virtual screening of the novel compounds from the ZINC database [33,34]. These novel compounds were further used for the screening of new inhibitors of RdRp of SARS-CoV-2. The validity of the screened compounds was checked by molecular docking approaches.

2.5. Drug likeness properties analysis of the screened compounds from ZINC database

SwissADME server was used to assess the Absorption, Distribution, Metabolism and Excretion (ADME) properties of the compounds screened from ZINC database [35]. This server is well known for successfully evaluating the pharmacokinetics, drug-likeness and medicinal chemistry friendliness of potential drug candidates. In this study, the physicochemical parameters (Formula Molecular weight, Molar Refractivity, TPSA), lipophilicity (Log Po/w (iLOGP), Log Po/w (XLOGP3), Log Po/w (WLOGP), Log Po/w (MLOGP), Log Po/w (SILICOS-IT), Consensus, Log Po/w), pharmacokinetic parameters (CYP1A2 inhibitor, CYP2C19 inhibitor, CYP2C9 inhibitor, CYP2D6 inhibitor, CYP3A4 inhibitor, Log Kp; skin permeation) and water solubility (Log S: SILICOS-IT, Solubility) were checked for the screened compounds considering all default parameters [36,37]. Additionally, OSIRIS Property Explorer and admetSAR were used to investigate the undesired effects of these compounds like mutagenicity, tumerogenecity and toxicity [38–41]. No ADME or toxicity analysis was required for the top selected drugs since the drugs were previously tested for FDA approval.

2.6. Evaluation of the docking performance

The docking results were further evaluated using two *in silico* techniques — i) re-docking of the selected inhibitors with other two docking tools such as PatchDock and *i*GEMDOCK, and ii) site-specific docking of these inhibitors against another PDB structure of RdRp of SARS-CoV-2 with the predicted binding site. PatchDock is an advanced molecular docking algorithm in which unacceptable penetration of receptor's atoms to ligand's atoms was discarded [42]. This algorithm has three major stages such as Molecular Shape Representation, Surface Patch Matching and Scoring with Filtering. *i*GEMDOCK is a molecular docking tool which employed generic evolutionary method for docking and specialized for pharmacological interactions [43]. In *i*GEMDOCK, the number of generation was set to 70 and the number of solution was 2. Further, the best-pose was selected for interaction analysis.

Additionally, the selected drugs and zinc compounds along with Remdesivir were allowed to dock against another structure of RdRp of SARS-COV-2 in a site-specific manner. The previously predicted binding site was set for this site-specific docking, and was carried out by Autodock Vina. Another crystal structure of RdRp of SAR-CoV-2 was retrieved from the Protein Data Bank (PDB) with PDB ID: 7BV2. After cleaning the structure with PyMOL, the structure was prepared for docking by Autodock tools. The grid box parameters were set to size 20 Å × 26 Å × 18 Å (x, y and z) and centre 117.203 Å × 90.242 Å × 76.951 Å (x, y and z).

2.7. Molecular dynamics simulation

Molecular dynamics (MD) simulation was performed in order to analyze the docked poses. In MD simulation, the integration of Newton's low generates successive iterations where the results specify how the positions and velocities of each molecule vary over time in a system [44]. In this study, MD simulation was performed for the top predicted

drug with lowest binding energy and the two predicted compounds from Zinc database. LARMD tools was adopted to run MD simulation considering the influence of water molecules and the time interval was set to 4 ns [45]. AMBER16 was used as the force field in this MD simulation where the Sander module was used to perform the minimization in 4 steps before the simulation [46]. The 2000 steps steepest descent method along with the 3000 steps conjugated gradient method were used in all minimization processes and the system was heated from 10 to 300 K in 30 ps. Finally, periodic boundary condition was applied to relax all the atoms in 300 K [45].

3. Results

3.1. Screening of RdRp inhibitors against the RdRp of SARS-CoV-2

Molecular docking of all the RNA polymerase inhibitors against RdRp of SARS-CoV-2 (PDB ID: 6M71) revealed Rifabutin, Rifapentine, Fidaxomicin, 7-methyl-guanosine-5′-triphosphate-5′-guanosineand Ivermectin chronologically as the top-most effective RdRp inhibitors of SARS-CoV-2 with highest binding affinity and lowest free energy (Table 1 and Fig. 1). Remarkably, all these top listed inhibitors showed lower binding energy compared to the positive control Remdesivir and Favipiravir. The whole molecular docking results were included in the Supplementary Table 2.

3.2. Structural insights of drug surface hotspot in the RdRp of SARS-CoV-2

The molecular docking pattern and amino acid residues involved were further analyzed to reveal the common interactive sites of RdRp in the SARS-CoV-2. Thus, the binding pattern of five most effective compounds along with Remdesivir and Favipiravir, were analyzed to observe the common drug surface hotspot. It was found that the amino acids Y32, K47, Y129, H133, N138, C139, T141 and S709 in RdRp were involved in the interaction with Rifabutin. The amino acids Y32, K47, Y129, H133 and S709 along with D140 and N781 were also found crucial for the RdRp of SARS-CoV-2 to interact with Rifapentine, Fidaxomicin, 7-methyl-guanosine-5′-triphosphate-5′-guanosine and Ivermectin (Table 1 and Figs. 2 and 3). Most surprisingly, these amino acid residues were also found to be involved in the interaction of Remdesivir (K47, Y129, A130, H133, F134, D135, N138, C139, T141, S709, T710, D711, Q773 and N781) and Favipiravir (Y129, H133, S709, K780 and N781).

3.3. Pharmacophore modeling and screening of ZINC database

The top listed RdRp inhibitors along with Remdesivir were further used for the pharmacophore modeling and screening of ZINC database. The pharmacophore modeling (predicted by the PharmaGIST) revealed 6 spatial features (Aromatic-1, Hydrophobic-1 and Acceptors-4) (Fig. 4). This pharmacophore model was imported in the ZINCPharmer for the screening of the ZINC Database, which revealed four different hits (ZINC09128258, ZINC09883305, ZINC09883308 and ZINC11286235). In addition, molecular docking analysis revealed that two compounds (ZINC09128258 and ZINC09883305) which are structural isomer of each other, could also act as the inhibitors of RdRp of SARS-CoV-2 as they showed similar binding pattern as the top drugs and controls (Table 2 and Figs. 5 and 6). However, these two compounds showed lower binding affinity than the top selected RdRp inhibitors. Additionally, higher number of non-covalent interactions was found for ZINC09883305 (9 non-covalent interactions). The chemical diagrams of all compounds analyzed in this study were shown in Fig. 7.

3.4. Drug likeness properties analysis of the screened compounds from ZINC 15 database

The physico-chemistry, pharmacokinetics, medicinal chemistry friendliness and toxicity of these two screened compounds (ZINC09128258 and ZINC09883305) from ZINC database were analyzed by SwissADME, ADMETsar and OSIRIS Property Explorer. The physiochemical parameters, lipophilicity and water solubility of these compounds are described in Table 3. Both compounds had some similar properties as they are structural isomer of each other. Water solubility was also studied in this study and it was found that all the compounds were moderately soluble. Other important properties such as Molecular weight (MW), molecular refractivity (MR) and topological polar surface area (TPSA), which are very useful for the estimation of ADME properties were also included in this study. Remarkably, none of the screened compounds showed any undesired effects such as mutagenicity, tumorigenicity, irritating and reproductive effects. However, these compounds showed CYP450 enzymes inhibition effects except CYP1A2. Lastly, BOILED-Egg model was employed to calculate the Blood-brain barrier (BBB) permeation that revealed no BBB permeate in the studied compounds [47].

3.5. Evaluation of the docking performance

Re-docking of the top five suggested drugs along with zinc compounds against the RdRp of SARS-CoV-2 using PatchDock and *i*GEMDOCK had mostly similar results as the previous results with Autodock Vina. In both tools, Rifabutin was found as the top most compound against RdRp with the lowest binding energy. Moreover, all the drugs were found to have the lowest binding energy than Remdesivir (Table 4). Additionally, site-specific docking against another structure with PDB ID 7BV2 revealed the binding affinity of all drugs were higher than Remdesivir and mostly similar as the previous blind docking against the structure with PDB ID 6M71 (Table 4). In this case, Fidaxomicin was found as the top most compound followed by Rifabutin and others.

Table 1
Top 5 RdRp inhibitors with binding energy and the amino acids involved in the interactions.

Sl. no.	Drug bank ID	Name	Binding energy (kcal/mol)	No of non-covalent interactions	Amino acids involved
1	DB00615	Rifabutin	−11.8	7	Y32, K47, Y129, H133, N138, C139, T141, S709
2	DB01201	Rifapentine	−11.6	10	V31, Y32, R33,K47, K121, Y122, Y129, H133, N138, C139, D140, T141, S709, N781
3	DB08874	Fidaxomicin	−10.9	16	Y32, K47, Y129, N131, H133, N138, D140, T141, S709, T710, D711, K714, N781, Q773
4	DB03958	7-methyl-guanosine-5′-triphosphate-5′-guanosine	−10	12	Y32, R33, K47,Y122, Y129, H133, D140, T141, A706, S709, T710, D711,, G774, N781
5	DB00602	Ivermectin	−9.9	9	Y32, L49, Y129, H133, S709, T710, K714, G774, N781
Control	DB14761	Remdesivir	−8.8	5	K47, Y129, A130, H133, F134, D135, N138, C139, T141, S709, T710, D711, Q773 and N781
Control	DB12466	Favipiravir	−5.3	6	Y129, H133, S709, K780 and N781

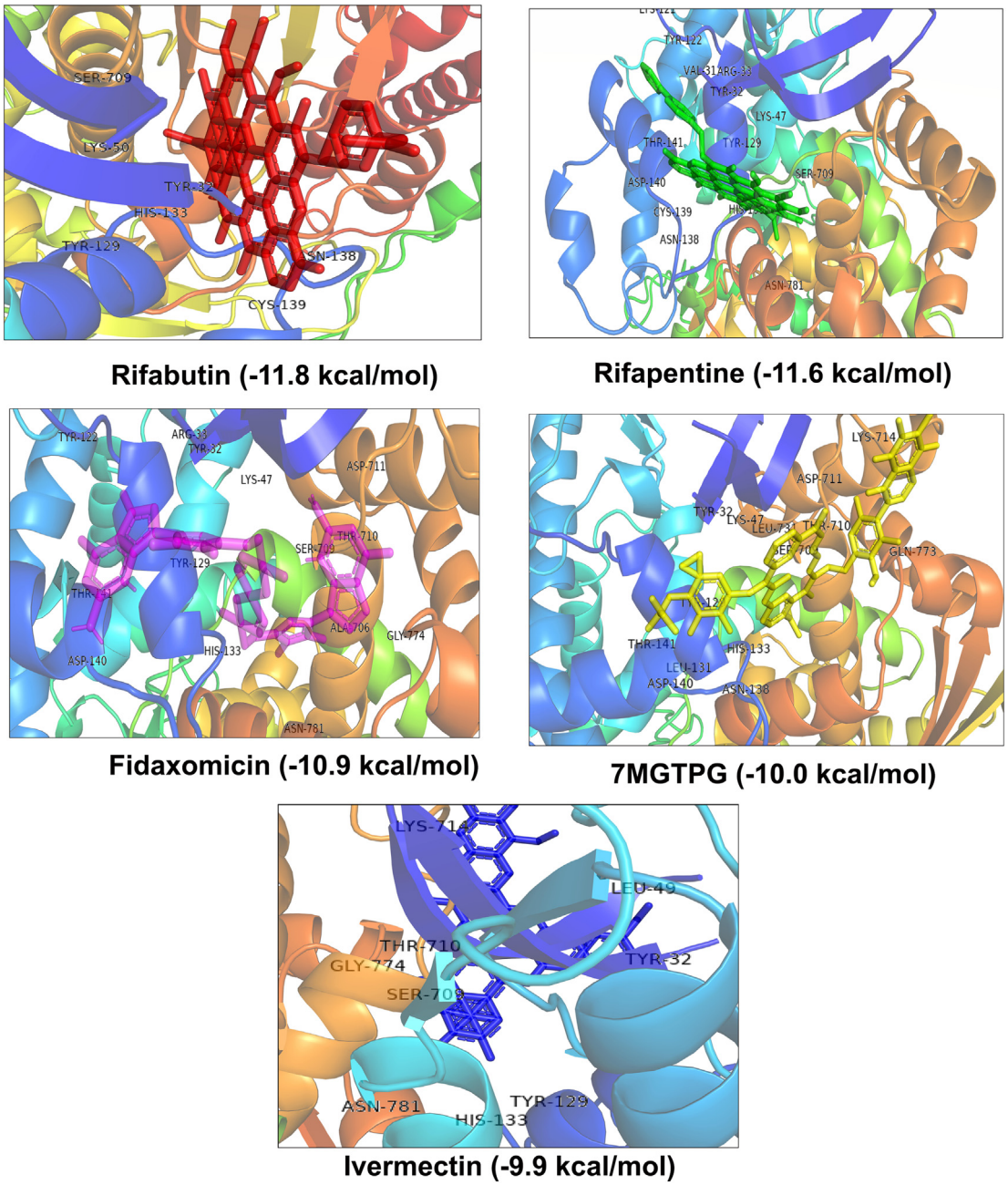

Fig. 1. Docked figures of Top 5 drug candidates with RdRp of SARS-CoV-2.

3.6. Molecular dynamics simulation

Molecular dynamics simulation was performed for the RdRp of SARS-CoV-2 in complex with Rifabutin and other two-screened compounds ZINC09128258 and ZINC09883305. Analysis of root mean square deviation (RMSD) showed that the receptor was in an equilibrium state before 1 ns after the binding of the inhibitors and the RMSD was less than 2 Å in all three complexes (Fig. 8). However, there was a much fluctuation found in RdRp for the complex with ZINC09883305. In case of Rifabutin-RdRp complex, both ligand and receptor sites amino acids are found in equilibrium state in 1 ns. Additionally, the number of H-bonds involved in the interactions between the inhibitors and the RdRp was also investigated during this simulation. An average of 2 hydrogen bonds was observed when the RdRp of SARS-CoV-2 in complex with rifabutin and ZINC09883305, while an average of 3 hydrogen bonds were found for ZINC09128258 in this 4 ns time interval (Fig. 9). However, all three complexes were found to have a maximum number of 5 hydrogen bonds.

In this study, the estimation of free energies consists of electrostatic energy (ELE), Van der Waals contribution (VDW), total gas phase energy (GAS) and final estimated binding energy (deltaPB/deltaGB). MM/PB (GB) SA calculations showed that the value of free energy in the RdRp in complex with Rifabutin, deltaPB ≈ −10.44 kcal/mol. Meanwhile, ZINC09128258 had the value of deltaPB ≈ −8.15 kcal/mol and ZINC09883305 had deltaPB ≈ −6.81 kcal/mol (Table 5).

Finally, Principal Component Analysis (PCA) was employed for the investigation of the effects of the conformational factors. This study found two distinct clusters for all three complexes in PC1 *vs* PC2 graph (Fig. 10). This graph has blue to red colored frames over time and represents the active and inactive state of a protein.

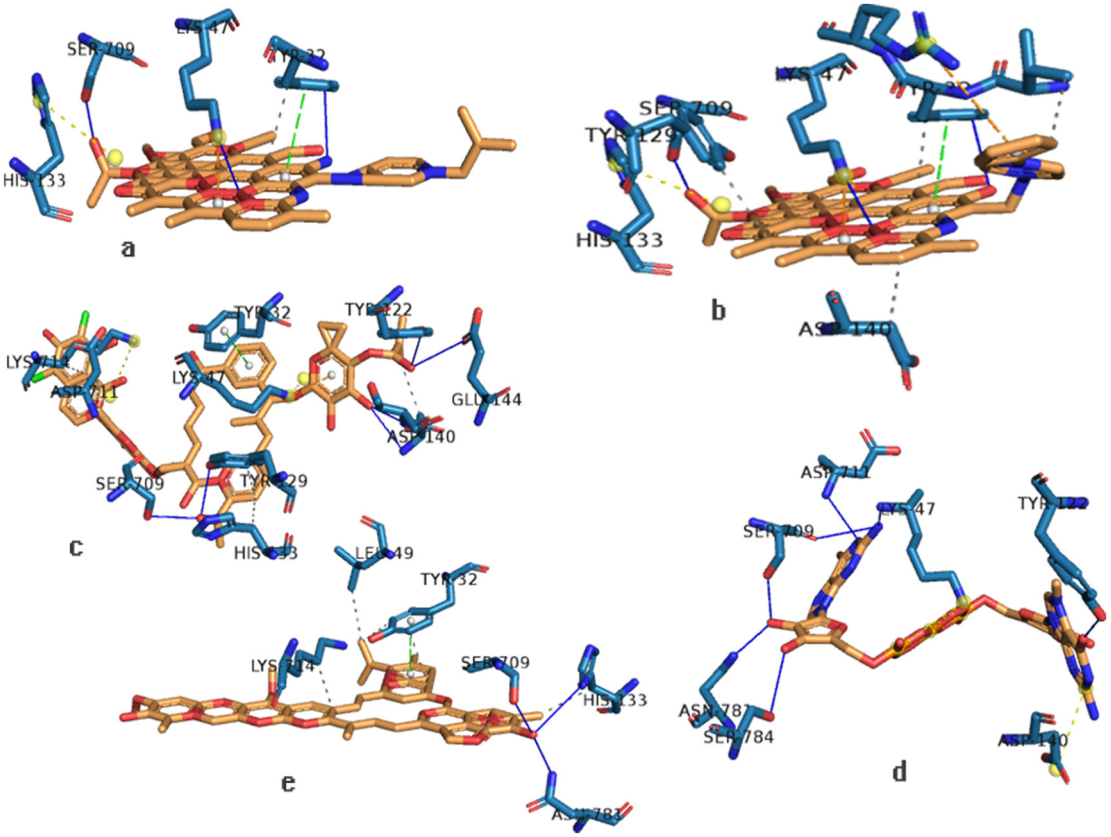

Fig. 2. The interaction of RdRp with (a) Rifabutin (b) Rifapentine (c) Fidaxomicin (d) 7-methyl-guanosine-5′-triphosphate-5′-guanosine and (e) Ivermectin. Here, drugs are in orange while protein active site pockets are in cyan lines. Solid blue lines represent H-bonds, while hydrophobic interactions are gray dashed lines. In addition, salt bridges, π-cation stacking, and halogen contacts are represented by yellow spheres connected by black dashed lines, orange dashed lines, and cyan lines, respectively.

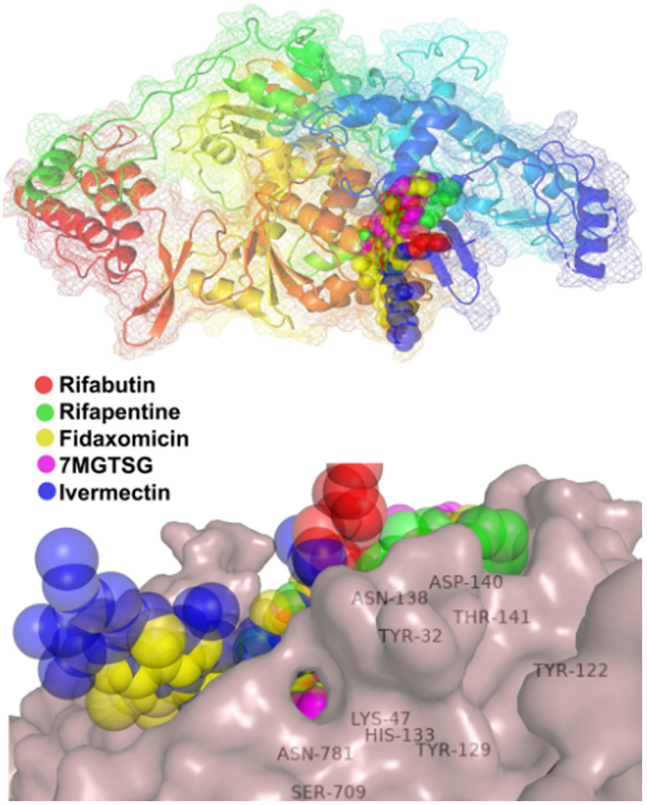

Fig. 3. Structural analysis of drug hotspot in RdRp of SARS-CoV-2.

4. Discussion

At present, COVID-19 is a global challenge for the scientific communities as its pandemic attitude is dangerously affecting millions of people and taking thousands of lives everyday. But to date, no satisfactory breakthrough has been made in the treatment of COVID-19 [48–51]. Several attempts have been made to treat this disease but these drug candidates remain questionable owing to low efficacy [52]. Computational approaches along with drug repurposing methods could be an effective approach to this COVID-19 challenge. In this study, several polymerase inhibitors targeting RdRp of SARS-CoV-2 were studied, as RdRp had already been shown to be an effective anti-viral drug target for various viral pathogens such as Hepatitis C Virus, HIV, Zika virus *etc.* [53,54]. Here, drug repurposing along with molecular docking was employed for the screening and analysis of the drug candidates against RdRp of SARS-CoV-2. Moreover, the common drug surface hotspot was

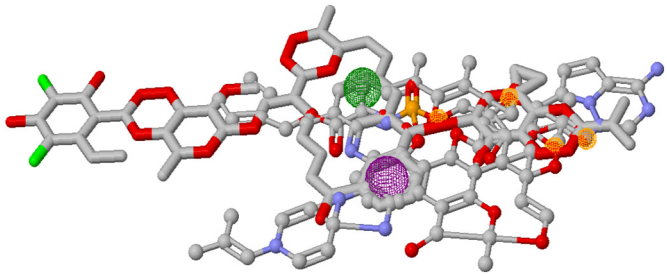

Fig. 4. Ligand-based pharmacophore model of RdRp of SARS-CoV-2. Here, green represents the hydrophobic features, violet represents aromatic features and yellow represents the hydrogen acceptor features.

Table 2
Molecular docking results of the screened compounds along with the amino acids involved in the interactions.

Sl. no.	ZINC ID	Compound IUPAC name	Binding energy kcal/mol	No. of non-covalent interactions	Amino acids involved
1	ZINC09128258	[(1,1-Dioxo-1λ^6-thiolan-3-yl)(2-methylpropyl)carbamoyl] methyl 3-(furan-2-amido)-4-methylbenzoate	−7.1	6	Y32, K47, H133, D135, A706, S709, T710. D711, K714, G774, N781, S784
2	ZINC09883305	[(Butan-2-yl)(1,1-dioxo-1λ^6-thiolan-3-yl)carbamoyl]methyl 3-(furan-2-amido)-4-methylbenzoate	−7	9	Y129, H133, D135, N138, A706, S709, T710, K780, N781, S784
Control	Drug Bank ID: DB14761	Drug name: Remdesivir	−8.8	5	K47, Y129, A130, H133, F134, D135, N138, C139, T141, S709, T710, D711, Q773 and N781
Control	Drug Bank ID: DB12466	Drug name: Favipiravir	−5.3	6	Y129, H133, S709, K780 and N781

studied along with modeling of pharmacophore which is very important for drug discovery. Additionally, novel compounds from ZINC database were screened out which could be developed as a new drug to treat COVID-19.

RdRp plays indispensable roles in the life cycle of RNA viruses. RNA viruses initiate RNA synthesis by virus polymerase utilizing primer-independent and primer-dependent mechanism. Moreover, RdRp based RNA synthesis doesn't occur in the mammalian cells offering an opportunity to design drugs specifically acting against RNA viruses. Additionally, the protein structure of RdRp in RNA viruses is found to be remarkably conserved. Various antiviral drugs have been developed targeting this enzyme for the treatment of infections caused by RNA viruses and they are working effectively [10,55].Therefore, this present study aimed to identify potential drugs targeting this enzyme for the treatment of COVID-19.

Molecular docking analysis revealed that Rifabutin, Rifapentine, Fidaxomicin, 7-methyl-guanosine-5′-triphosphate-5′-guanosine and Ivermectin could be potential RdRp inhibitors of SARS-CoV-2. Notably, Ivermectin has already been reported as showing inhibitor property in SARS-CoV-19 replications *in vitro* [56]. Rifabutin and Rifabutin have also been reported for their anti-viral activity against HIV and *vaccinia virus* respectively [57,58]. Moreover, the vast number of non-covalent

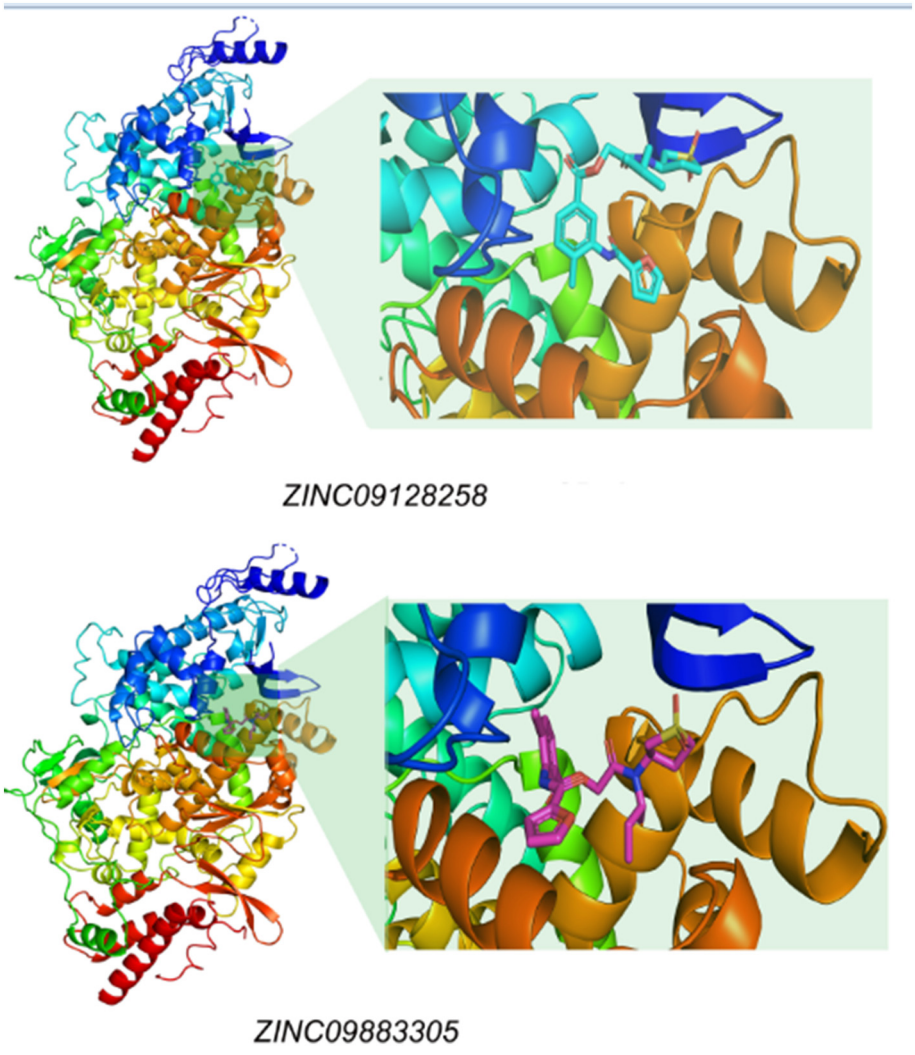

Fig. 5. Docked figures of selected ZINC compounds with RdRp of SARS-CoV-2.

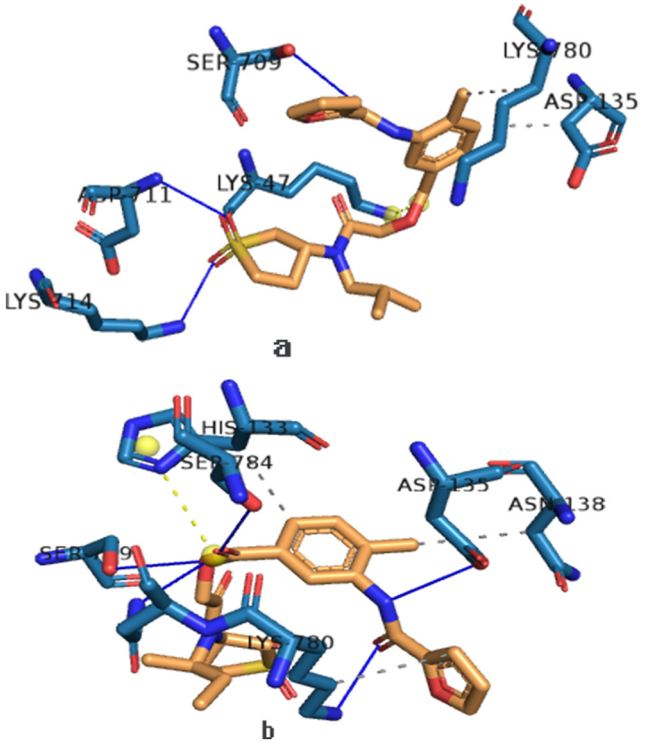

Fig. 6. The interaction of RdRp with (a) ZINC09128258 and (b) ZINC09883305. Here, drugs are in orange while protein active site pockets are in cyan lines. Solid blue lines represent H-bonds, while hydrophobic interactions are gray dashed lines. In addition, salt bridges, π-cation stacking, and halogen contacts are represented by yellow spheres connected by black dashed lines, orange dashed lines, and cyan lines, respectively.

interactions between these screened compounds with RdRp suggests that the protein-inhibitor complexes are very stable. In addition to these drugs, Remdesivir along with Favipiravir which has already been suggested for the treatment of COVID-19, was also found to be effective as the inhibitor of RdRp of SARS-CoV-2 [14]. Although their binding affinity was lower than the aforementioned top five drugs, the binding pattern was almost similar to these drugs. The drug surface hotspot study revealed that the molecular binding sites of all the five compounds were of a similar pattern that could be the hotspot of drug binding to the RdRp of SARS-CoV-2. This study suggested that amino acids Y32, K47, Y122, Y129, H133, N138, D140, T141, S709 and N781 in RdRp of SARS-CoV-2 could make effective interactions with drugs, though this needs to be validated in wet lab. Additionally, pharmacophore was designed using the top RdRp inhibitor drugs along with Remdesivir, which was used further for the screening of ZINC database. Molecular docking analysis revealed that two compounds among the four hits had interacted effectively with the RdRp of SARS-CoV-2 which is indicative of their potential as inhibitors of the enzyme. Although their binding affinity was lower than one control (Remdesivir), the vast number of interactions would give the complex its stability with this binding energy. Moreover, ADME and toxicity analysis of these compounds suggested that they could be used for the development of new drugs to treat COVID-19. However, the study of the inhibition of cytochromes P450 (CYP) isoforms revealed that there was a possibility that the suggested compounds could interact with CYP isoforms.

Evaluation of the docking performance is very crucial to make the prediction more strong. Re-docking with other docking tools and site-specific docking with another structure are very effective ways of the evaluation of the docking results [59]. In this study, re-docking provided the mostly similar docking results and Rifabutin was found to have the highest binding affinity in all tools. All the drugs were found to have much higher binding affinity than the control. However, the scores

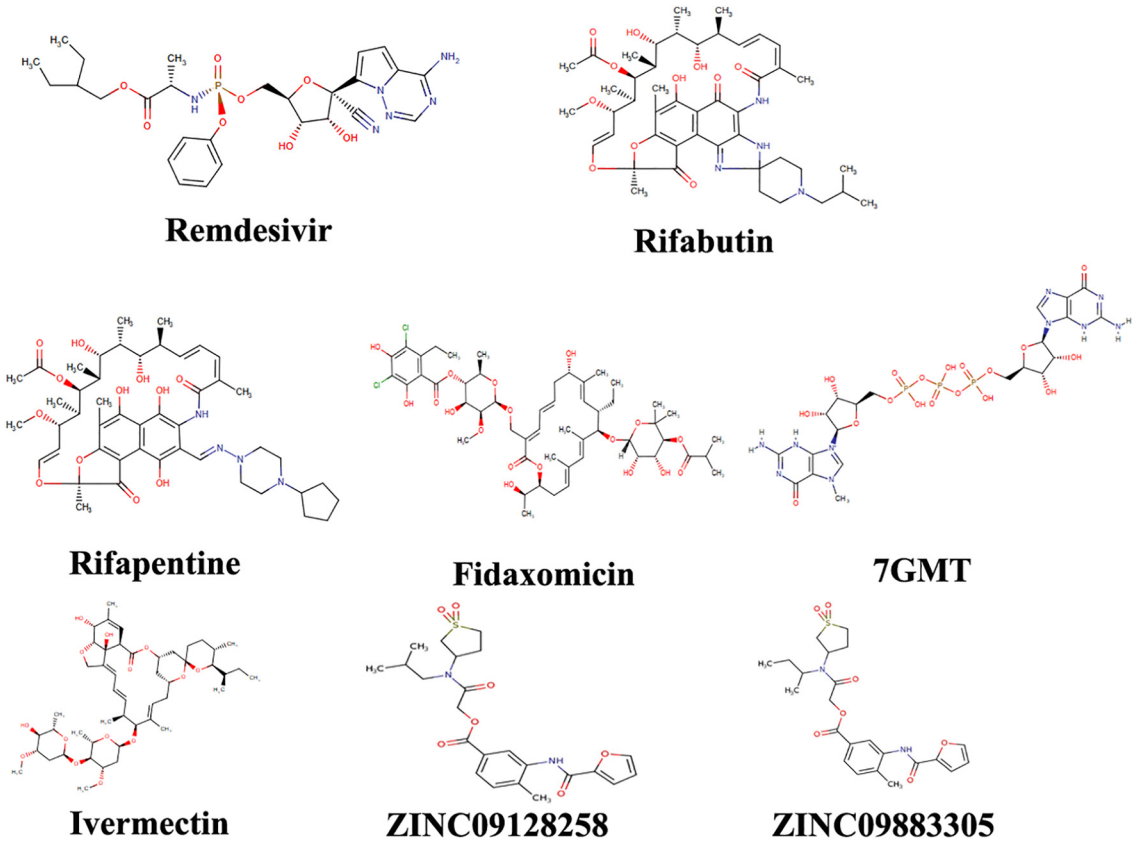

Fig. 7. The chemical diagrams of all compounds analyzed in this study.

Table 3
Drug likeness properties analysis of screened compounds from ZINC 15 database.

Properties	ZINC09128258	ZINC09883305
General		
Formula	$C_{23}H_{28}N_2O_7S$	$C_{23}H_{28}N_2O_7S$
Molecular weight (g/mol)	476.54	476.54
Molar refractivity	122.38	122.38
TPSA (topological polar surface area)	131.37	131.37
Lipophilicity		
Log $P_{o/w}$ (iLOGP)	3.15	3.01
Log Po/w (XLOGP3)	2.8	2.8
Log Po/w (WLOGP)	3.56	3.7
Log Po/w (MLOGP)	1.28	1.28
Log Po/w (SILICOSNoIT)	2.62	2.62
Consensus Log Po/w	2.68	2.68
Solubility		
LOG S (SILICOS-IT)	−5.77	−5.77
SILICOS-IT Solubility (mg/ml)	8.02E−04	8.02E−04
SILICOS-IT Solubility (mol/l)	1.68E−06	1.68E−06
Solubility class	Moderately soluble	Moderately soluble
Pharmacokinetics		
Druglikeness	−3.39	1.84
Drug-score	0.34	0.6
Blood-brain-barrier permeant	No	No
Human intestinal absorption	Yes	Yes
Caco-2 permeant	No	No
P-glycoprotein substrate	No	Yes
CYP450 1A2 inhibitor	No	No
CYP450 2C9 inhibitor	Yes	Yes
CYP450 2D6 inhibitor	Yes	Yes
CYP450 2C19 inhibitor	Yes	Yes
CYP450 3A4 inhibitor	Yes	Yes
CYP inhibitory promiscuity	Yes	Yes
Toxicity		
AMES toxicity	No	No
Carcinogens	No	No
Biodegradation	No	No
Acute oral toxicity (kg/mol)	III, 2.787	III, 2.731
Mutagenicity	No	No
Tumorigenicity	No	No
Irritating effects	No	No
Reproductive effects	No	No

were different as different methods use different scoring functions. Additionally, site-specific docking against another structure of RdRp revealed the mostly same binding poses and the binding affinity.

The accurate prediction of protein-inhibitors complexes is very important for the drug development by the computational approaches. MD simulation could be used in the assessment of the docking pose predicted through the molecular docking analysis. It could be predicted whether a docked pose is stable or not in an aqueous environment [60]. In this study, MD simulation was also adopted to assess the stability of Rifabutin-RdRp, ZINC09128258-RdRp and ZINC09883305-RdRp complexes by using the following descriptors: ligand-receptor RMSD,

Table 4
Evaluation of the docking performance.

Name	Site-specific docking with 7BV2	PatchDock score	i-GEMDOCK score
Rifabutin	−10.3	−212.63	−136.88
Rifapentine	−9.8	−129.74	−114.29
Fldaxomicin	−11	−119.9	−112.45
7MGT	−8.9	−112.34	−129.24
Ivermectin	−9.2	−119.79	−112.19
ZINC09128258	−7.6	−143.23	−85.98
ZINC09883305	−6.6	−55.25	−91.36
Remdesivir	−8.7	−72.72	−111.18

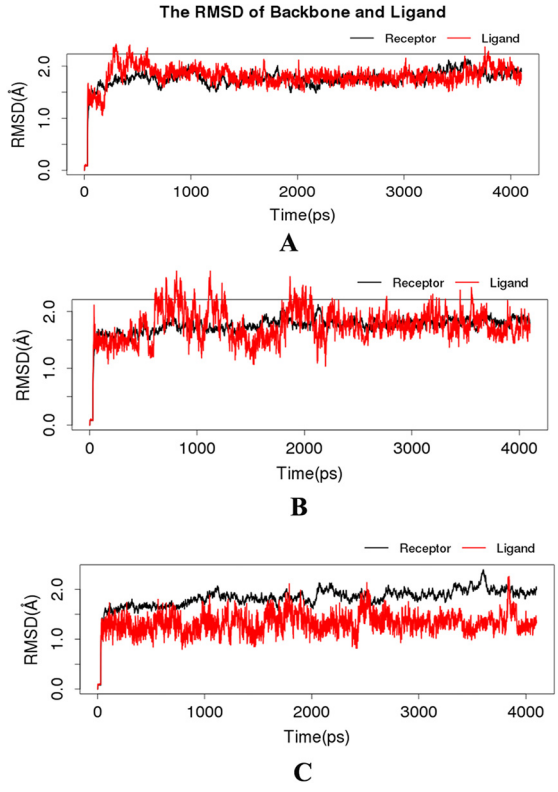

Fig. 8. RMSD values of protein-inhibitor complexes over the simulation time. Here, RdRp is in complex with (A) Rifabutin, (B) ZINC09128258, and (C) ZINC09883305.

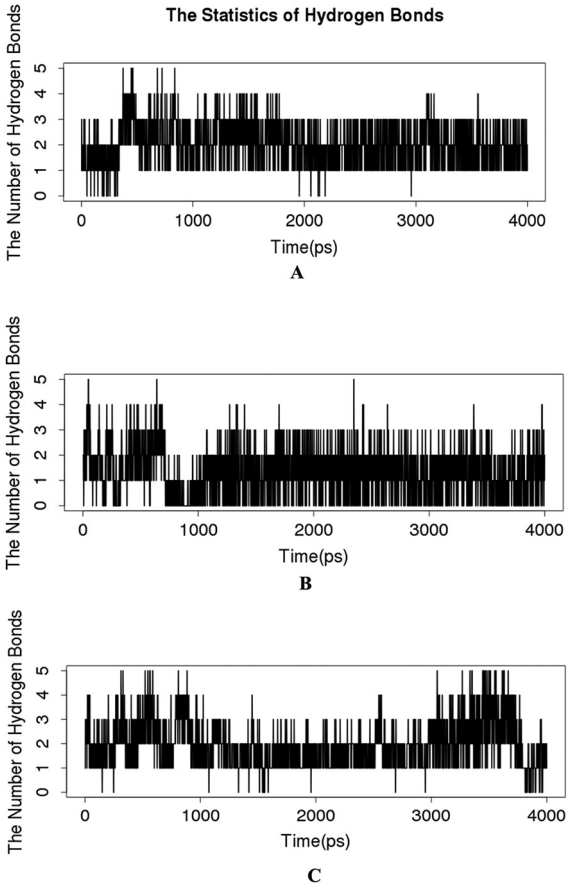

Fig. 9. Number of H-bonds involved in the interaction between protein and inhibitors during the MD simulation. Here, RdRp is in complex with (A) Rifabutin, (B) ZINC09128258, and (C) ZINC09883305.

Table 5
MM/PB(*GB*)SA binding free energies (in kcal/mol) of inhibitors in complex with RdRp of SARS-CoV-2.

Inhibitors	ELE	VDW	GAS	deltaPB	deltaGB
Rifabutin	−14.12	−39.39	−53.35	−10.44	−9.67
ZINC09128258	−13.07	−35.01	−48.08	−8.15	−12.41
ZINC09883305	−19.47	−47.16	−67.10	−6.81	−13.86

number of H-bonds, calculation of MM/PB(*GB*)SA binding free energies and PCA. The RMSD of receptor in complex with the inhibitors was found to be below 2 Å for all three complexes indicating the high stability of the complexes. Moreover, H-bond analysis revealed that the H-bonds were stable over the entire simulation and would probably play a significant role in stabilizing the complexes. By the calculation of MM/PB(*GB*)SA binding free energies, the value was found to be consistent with docking results. Additionally, Principal Component Analysis (PCA) revealed that all three inhibitors Rifabutin, ZINC09128258 and ZINC09883305 responded very well with a greater degree of inactivity of the RdRp of SARS-CoV-2. Two distinct clusters were found for all three complexes which provide insights into the large conformational change in the RdRp through the binding of the inhibitors. These all findings through the MD simulation strengthened our docking prediction.

5. Conclusion

COVID-19 has created a disastrous global crisis affecting thousands of people every day, having already claimed thousands of lives, and severely hampered the global economy. The present study aimed to combat this global crisis by suggesting potential drug candidates for the treatment of COVID-19. Rifabutin, Rifapentine, Fidaxomicin, 7-methylguanosine-5′-triphosphate-5′-guanosine, Ivermectin and other screened novel compounds made the common drug surface hotspot in the RdRp of SARS-CoV-2, suggesting strongly that they could be effective in the treatment of SARS-CoV-2.

Supplementary data to this article can be found online at https://doi.org/10.1016/j.ijbiomac.2020.09.098.

Ethical approval

Not required.

Funding

No specific grant was received for this study. MH receives grant support from the (1) Research Center, Shahjalal University of Science and Technology, (2) Bangladesh Bureau of Educational Information and Statistics, and the (3) Ministry of Education, Government of Bangladesh.

Data availability

All data supporting the findings of this study are available within the article and its supplementary materials.

CRediT authorship contribution statement

Md. Sorwer Alam Parvez: Conceptualization, Methodology, Software, Data curation, Visualization, Writing - original draft. **Md. Adnan Karim:** Methodology, Software, Data curation, Visualization. **Mahmudul Hasan:** Visualization, Investigation. **Jomana Jaman:** Software. **Ziaul Karim:** Validation. **Tohura Tahsin:** Writing - review & editing. **Md. Nazmul Hasan:** Supervision. **Mohammad Jakir Hosen:** Supervision, Writing - review & editing.

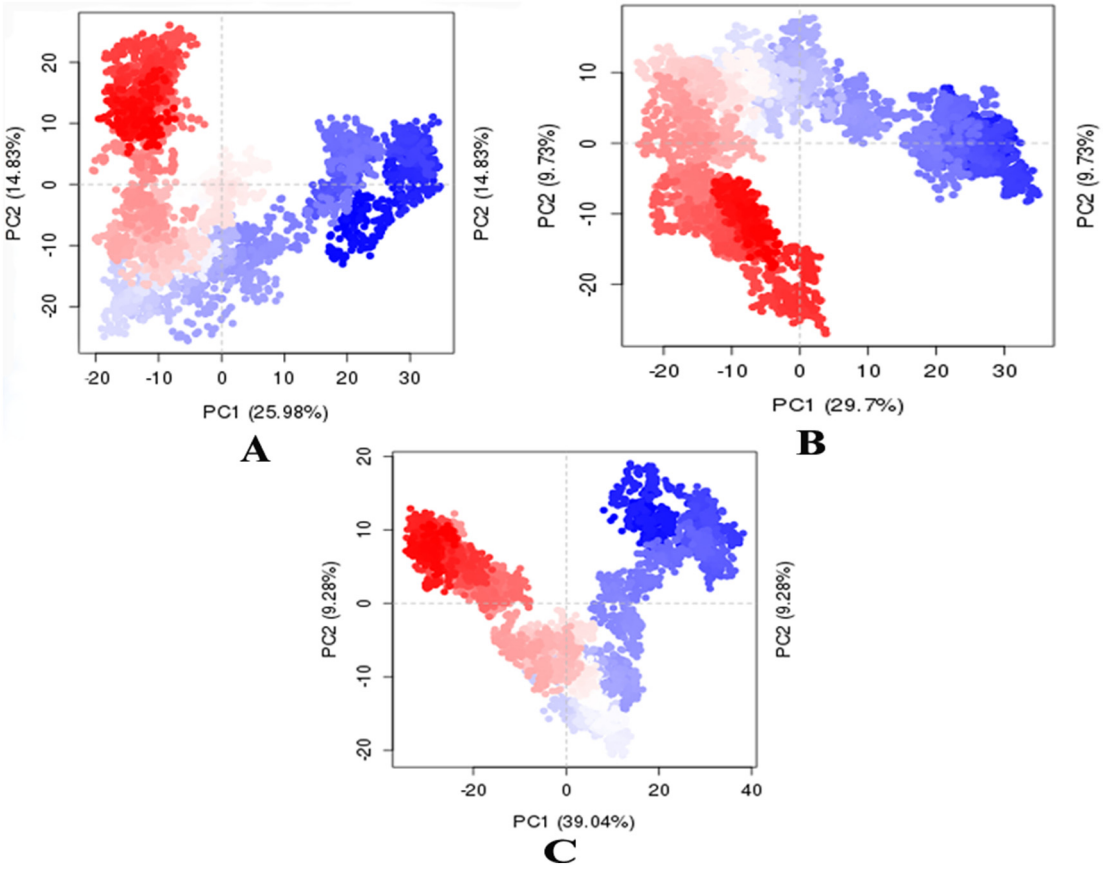

Fig. 10. PCA results trejectories for the protein-inhibitor complexes. Here, RdRp in complex with (A) Rifabutin, (B) ZINC09128258, and (C) ZINC098833. In this graph, the colour blue to red frames over time.

Declaration of competing interest

The authors declare that they have no competing interests.

References

[1] R. Porcheddu, C. Serra, D. Kelvin, N. Kelvin, S. Rubino, Similarity in case fatality rates (CFR) of COVID-19/SARS-COV-2 in Italy and China, J. Infect. Dev. Count. 14 (2020) 125–128, https://doi.org/10.3855/jidc.12600.

[2] Worldometer, Coronavirus Cases, Worldometer, 2020 1–22, https://doi.org/10.1101/2020.01.23.20018549V2.

[3] WHO, Coronavirus Disease (COVID-19) Situation Dashboard, 2020.

[4] J.F.W. Chan, S. Yuan, K.H. Kok, K.K.W. To, H. Chu, J. Yang, F. Xing, J. Liu, C.C.Y. Yip, R.W.S. Poon, H.W. Tsoi, S.K.F. Lo, K.H. Chan, V.K.M. Poon, W.M. Chan, J.D. Ip, J.P. Cai, V.C.C. Cheng, H. Chen, C.K.M. Hui, K.Y. Yuen, A familial cluster of pneumonia associated with the 2019 novel coronavirus indicating person-to-person transmission: a study of a family cluster, Lancet (2020)https://doi.org/10.1016/S0140-6736(20)30154-9.

[5] N. Chen, M. Zhou, X. Dong, J. Qu, F. Gong, Y. Han, Y. Qiu, J. Wang, Y. Liu, Y. Wei, J. Xia, T. Yu, X. Zhang, L. Zhang, Epidemiological and clinical characteristics of 99 cases of 2019 novel coronavirus pneumonia in Wuhan, China: a descriptive study, Lancet (2020)https://doi.org/10.1016/S0140-6736(20)30211-7.

[6] Y. Yang, Q. Lu, M. Liu, Y. Wang, A. Zhang, N. Jalali, N. Dean, I. Longini, M.E. Halloran, B. Xu, X. Zhang, L. Wang, W. Liu, L. Fang, Epidemiological and clinical features of the 2019 novel coronavirus outbreak in China, MedRxiv (2020)https://doi.org/10.1101/2020.02.10.20021675 2020.02.10.20021675.

[7] A.-2019-nCoV Volunteers, Z. Li, M. Wu, J. Guo, J. Yao, X. Liao, S. Song, M. Han, J. Li, G. Duan, Y. Zhou, X. Wu, Z. Zhou, T. Wang, M. Hu, X. Chen, Y. Fu, C. Lei, H. Dong, Y. Zhou, H. Jia, X. Chen, J. Yan, Caution on kidney dysfunctions of 2019-nCoV patients, MedRxiv (2020)https://doi.org/10.1101/2020.02.08.20021212 2020.02.08.20021212.

[8] M. Pal, G. Berhanu, C. Desalegn, V. Kandi, Severe acute respiratory syndrome Coronavirus-2 (SARS-CoV-2): an update, Cureus 12 (2020)https://doi.org/10.7759/cureus.7423.

[9] A. Zumla, J.F.W. Chan, E.I. Azhar, D.S.C. Hui, K.Y. Yuen, Coronaviruses—drug discovery and therapeutic options, Nat. Rev. Drug Discov. 15 (2016) 327–347, https://doi.org/10.1038/nrd.2015.37.

[10] A.A. Elfiky, Ribavirin, Remdesivir, Sofosbuvir, Galidesivir, and Tenofovir against SARS-CoV-2 RNA dependent RNA polymerase (RdRp): a molecular docking study, Life Sci. (2020) 117592, https://doi.org/10.1016/j.lfs.2020.117592.

[11] J. Lung, Y. Lin, Y. Yang, Y. Chou, L. Shu, Y. Cheng, H. Te Liu, C. Wu, The potential chemical structure of anti-SARS-CoV-2 RNA-dependent RNA polymerase, J. Med. Virol. (2020) jmv.25761, https://doi.org/10.1002/jmv.25761.

[12] G. Li, E. De Clercq, Therapeutic options for the 2019 novel coronavirus (2019-nCoV), Nat. Rev. Drug Discov. 19 (2020) 149–150, https://doi.org/10.1038/d41573-020-00016-0.

[13] Y. Furuta, B.B. Gowen, K. Takahashi, K. Shiraki, D.F. Smee, D.L. Barnard, Favipiravir (T-705), a novel viral RNA polymerase inhibitor, Antivir. Res. 100 (2013) 446–454, https://doi.org/10.1016/j.antiviral.2013.09.015.

[14] M. Wang, R. Cao, L. Zhang, X. Yang, J. Liu, M. Xu, Z. Shi, Z. Hu, W. Zhong, G. Xiao, Remdesivir and chloroquine effectively inhibit the recently emerged novel coronavirus (2019-nCoV) in vitro, Cell Res. 30 (2020) 269–271, https://doi.org/10.1038/s41422-020-0282-0.

[15] M.L. Agostini, E.L. Andres, A.C. Sims, R.L. Graham, T.P. Sheahan, X. Lu, E.C. Smith, J.B. Case, J.Y. Feng, R. Jordan, A.S. Ray, T. Cihlar, D. Siegel, R.L. Mackman, M.O. Clarke, R.S. Baric, M.R. Denison, Coronavirus susceptibility to the antiviral remdesivir (GS-5734) is mediated by the viral polymerase and the proofreading exoribonuclease, MBio 9 (2018)https://doi.org/10.1128/mBio.00221-18.

[16] L. Zhang, R. Zhou, Binding Mechanism of Remdesivir to SARS-CoV-2 RNA Dependent RNA Polymerase, 2020https://doi.org/10.20944/preprints202003.0267.v1.

[17] C. Harrison, Coronavirus puts drug repurposing on the fast track, Nat. Biotechnol. (2020)https://doi.org/10.1038/d41587-020-00003-1.

[18] S. Ekins, J. Mestres, B. Testa, In silico pharmacology for drug discovery: methods for virtual ligand screening and profiling, Br. J. Pharmacol. 152 (2007) 9–20, https://doi.org/10.1038/sj.bjp.0707305.

[19] R.E. Hubbard, I. Chen, B. Davis, Informatics and modeling challenges in fragment-based drug discovery, Curr. Opin. Drug Discov. Dev. 10 (2007) 289–297.

[20] A. Pizzorno, B. Padey, O. Terrier, M. Rosa-Calatrava, Drug repurposing approaches for the treatment of influenza viral infection: reviving old drugs to fight against a long-lived enemy, Front. Immunol. 10 (2019)https://doi.org/10.3389/fimmu.2019.00531.

[21] B. Mercorelli, G. Palù, A. Loregian, Drug repurposing for viral infectious diseases: how far are we? Trends Microbiol. 26 (2018) 865–876, https://doi.org/10.1016/j.tim.2018.04.004.

[22] X. Li, J. Yu, Z. Zhang, J. Ren, A.E. Peluffo, W. Zhang, Y. Zhao, K. Yan, D. Cohen, W. Wang, Network Bioinformatics Analysis Provides Insight Into Drug Repurposing for COVID-2019, 2020https://doi.org/10.20944/preprints202003.0286.v1.

[23] N.C.B.I. Resource Coordinators, Database resources of the National Center for Biotechnology Information, Nucleic Acids Res. 44 (2016) D7–19, https://doi.org/10.1093/nar/gkv1290.

[24] P.W. Rose, A. Prlić, A. Altunkaya, C. Bi, A.R. Bradley, C.H. Christie, L. Di Costanzo, J.M. Duarte, S. Dutta, Z. Feng, R.K. Green, D.S. Goodsell, B.P. Hudson, T. Kalro, R. Lowe, E. Peisach, C. Randle, A.S. Rose, C. Shao, Y.-P. Tao, Y. Valasatava, M. Voigt, J.D. Westbrook, J. Woo, H. Yang, J. Young, C. Zardecki, H.M. Berman, S.K. Burley, The RCSB protein data bank: integrative view of protein, gene and 3D structural information, Nucleic Acids Res. 45 (2017) D271–D281.

[25] D.S. Wishart, Y.D. Feunang, A.C. Guo, E.J. Lo, A. Marcu, J.R. Grant, T. Sajed, D. Johnson, C. Li, Z. Sayeeda, N. Assempour, I. Iynkkaran, Y. Liu, A. Maciejewski, N. Gale, A. Wilson, L. Chin, R. Cummings, D. Le, A. Pon, C. Knox, M. Wilson, DrugBank 5.0: a major update to the DrugBank database for 2018, Nucleic Acids Res. 46 (2018) D1074–D1082, https://doi.org/10.1093/nar/gkx1037.

[26] O. Trott, A.J. Olson, AutoDock Vina: improving the speed and accuracy of docking with a new scoring function, efficient optimization, and multithreading, J. Comput. Chem. 31 (2009)https://doi.org/10.1002/jcc.21334 NA-NA.

[27] W.L. DeLano, Pymol: an open-source molecular graphics tool, CCP4 Newsl Prot. Crystallogr 40 (1) (2002) 82–92.

[28] R.A. Laskowski, M.B. Swindells, LigPlot+: multiple ligand-protein interaction diagrams for drug discovery, J. Chem. Inf. Model. 51 (2011) 2778–2786, https://doi.org/10.1021/ci200227u.

[29] D.S. Biovia, Discovery Studio Modeling Environment, Release 2017, Dassault Systèmes, San Diego, 2016.

[30] S. Salentin, S. Schreiber, V.J. Haupt, M.F. Adasme, M. Schroeder, PLIP — fully automated protein-ligand interaction profiler, Nucleic Acids Res. 43 (2015) W443–W447, https://doi.org/10.7490/F1000RESEARCH.1098304.1.

[31] D. Schneidman-Duhovny, O. Dror, Y. Inbar, R. Nussinov, H.J. Wolfson, Deterministic pharmacophore detection via multiple flexible alignment of drug-like molecules, J. Comput. Biol. 15 (2008) 737–754, https://doi.org/10.1089/cmb.2007.0130.

[32] D. Schneidman-Duhovny, O. Dror, Y. Inbar, R. Nussinov, H.J. Wolfson, PharmaGist: a webserver for ligand-based pharmacophore detection, Nucleic Acids Res. 36 (2008) W223–W228, https://doi.org/10.1093/nar/gkn187.

[33] D.R. Koes, C.J. Camacho, ZINCPharmer: pharmacophore search of the ZINC database, Nucleic Acids Res. 40 (2012) W409–W414, https://doi.org/10.1093/nar/gks378.

[34] J.J. Irwin, B.K. Shoichet, ZINC — a free database of commercially available compounds for virtual screening, J. Chem. Inf. Model. 45 (2005) 177–182, https://doi.org/10.1021/ci049714+.

[35] A. Daina, O. Michielin, V. Zoete, SwissADME: a free web tool to evaluate pharmacokinetics, drug-likeness and medicinal chemistry friendliness of small molecules, Sci. Rep. 7 (2017), 42717, https://doi.org/10.1038/srep42717.

[36] P. Tripathi, S. Ghosh, S.N. Talapatra, Bioavailability prediction of phytochemicals present in Calotropis procera (Aiton) R. Br. by using Swiss-ADME tool, World Sci. News 131 (2019) 147–163.

[37] S. Mishra, R. Dahima, In vitro ADME studies of TUG-891, a GPR-120 inhibitor using SWISS ADME predictor, J. Drug Deliv. Ther. 9 (2019) 366–369, https://doi.org/10.22270/jddt.v9i2-s.2710.

[38] Molecular Properties Prediction — Osiris Property Explorer2020.

[39] J. Shen, F. Cheng, Y. Xu, W. Li, Y. Tang, Estimation of ADME properties with substructure pattern recognition, J. Chem. Inf. Model. 50 (2010) 1034–1041, https://doi.org/10.1021/ci100104j.

[40] C. Xu, F. Cheng, L. Chen, Z. Du, W. Li, G. Liu, P.W. Lee, Y. Tang, In silico prediction of chemical ames mutagenicity, J. Chem. Inf. Model. 52 (2012) 2840–2847, https://doi.org/10.1021/ci300400a.

[41] X. Li, Z. Du, J. Wang, Z. Wu, W. Li, G. Liu, X. Shen, Y. Tang, In silico estimation of chemical carcinogenicity with binary and ternary classification methods, Mol. Inform. 34 (2015) 228–235, https://doi.org/10.1002/minf.201400127.

[42] D. Schneidman-duhovny, Y. Inbar, R. Nussinov, H.J. Wolfson, PatchDock and SymmDock : Servers for Rigid and Symmetric Docking, vol. 33, 2005 363–367, https://doi.org/10.1093/nar/gki481.

[43] K. Hsu, Y. Chen, S. Lin, J. Yang, iGEMDOCK: A Graphical Environment of Enhancing GEMDOCK Using Pharmacological Interactions and Post-screening Analysis, vol. 12, 2011 1–11.

[44] A.R. Leach, Molecular Modelling: Principles and Applications, 2nd ed. Pearson Education, 2001.

[45] J. Yang, F. Wang, Y. Chen, G. Hao, G. Yang, LARMD : Integration of Bioinformatic Resources to Profile Ligand-driven Protein Dynamics With a Case on the Activation of Estrogen Receptor, vol. 00, 2019 1–13, https://doi.org/10.1093/bib/bbz141.

[46] D.A. Case, T.E. Cheatham, T.O.M. Darden, H. Gohlke, R.A.Y. Luo, K.M. Merz, A. Onufriev, C. Simmerling, B. Wang, R.J. Woods, The Amber Biomolecular Simulation Programs, 12255, 2005https://doi.org/10.1002/jcc.20290.

[47] A. Daina, V. Zoete, A BOILED-egg to predict gastrointestinal absorption and brain penetration of small molecules, ChemMedChem 11 (2016) 1117–1121, https://doi.org/10.1002/cmdc.201600182.

[48] M.A. Lake, What we know so far: COVID-19 current clinical knowledge and research, Clin. Med. 20 (2020) 124–127, https://doi.org/10.7861/clinmed.2019-coron.

[49] K.S. Yuen, Z.W. Ye, S.Y. Fung, C.P. Chan, D.Y. Jin, SARS-CoV-2 and COVID-19: the most important research questions, Cell Biosci 10 (2020) 40, https://doi.org/10.1186/s13578-020-00404-4.

[50] Y. Fang, H. Zhang, J. Xie, M. Lin, L. Ying, P. Pang, W. Ji, Sensitivity of chest CT for COVID-19: comparison to RT-PCR, Radiology. (2020) 200432, https://doi.org/10.1148/radiol.2020200432.

[51] L. Dong, S. Hu, J. Gao, Discovering drugs to treat coronavirus disease 2019 (COVID-19), Drug Discov. Ther. 14 (2020) 58–60, https://doi.org/10.5582/ddt.2020.01012.

[52] D. Zhou, S.-M. Dai, Q. Tong, COVID-19: a recommendation to examine the effect of hydroxychloroquine in preventing infection and progression, J. Antimicrob. Chemother. (2020)https://doi.org/10.1093/jac/dkaa114.

[53] E. De Clercq, The design of drugs for HIV and HCV, Nat. Rev. Drug Discov. 6 (2007) 1001–1018, https://doi.org/10.1038/nrd2424.

[54] H.-T. Xu, S.A. Hassounah, S.P. Colby-Germinario, M. Oliveira, C. Fogarty, Y. Quan, Y. Han, O. Golubkov, I. Ibanescu, B. Brenner, B.R. Stranix, M.A. Wainberg, Purification of Zika virus RNA-dependent RNA polymerase and its use to identify small-molecule Zika inhibitors, J. Antimicrob. Chemother. 72 (2017) 727–734, https://doi.org/10.1093/jac/dkw514.

[55] A. Ganeshpurkar, G. Gutti, S.K. Singh, RNA-dependent RNA polymerases and their emerging roles in antiviral therapy, Viral Polym. Elsevier 2019, pp. 1–42, https://doi.org/10.1016/b978-0-12-815422-9.00001-2.

[56] L. Caly, J.D. Druce, M.G. Catton, D.A. Jans, K.M. Wagstaff, The FDA-approved drug Ivermectin inhibits the replication of SARS-CoV-2 in vitro, Antivir. Res. (2020) 104787, https://doi.org/10.1016/j.antiviral.2020.104787.

[57] B. Polsky, Antiviral chemotherapy for infection with human immunodeficiency virus, Rev. Infect. Dis. 11 (1989) S1648–S1663, https://doi.org/10.1093/CLINIDS/11.SUPPLEMENT_7.S1648.

[58] M.N. Prichard, E.R. Kern, Orthopoxvirus targets for the development of antiviral therapies, Curr. Drug Targets. Infect. Disord. 5 (2005) 17–28, https://doi.org/10.2174/1568005053174627.

[59] P. Agrawal, H. Singh, H.K. Srivastava, S. Singh, G. Kishore, G.P.S. Raghava, Benchmarking of Different Molecular Docking Methods for Protein-Peptide Docking, vol. 19, 2019.

[60] H. Sakano, Takako, Md Iqbal Mahamood, Takefumi Yamashita, Fujitani, Molecular dynamics analysis to evaluate docking pose prediction, Biophys. Physicobiol. 13 (2016) 181–194, https://doi.org/10.2142/biophysico.13.0.